Eur Biophys J (1990) 18:25–32

European Biophysics Journal

Sodium ionic and gating currents in mammalian cells

O. Moran [1, 2] **and F. Conti** [2]

[1] Scuola Internazionale Superiore de Studi Avanzati (SISSA), Strada Costiera 11, I-34014 Trieste, Italy
[2] Istituto di Cibernetica e Biofisica C.N.R., Via Dodecaneso 33, I-16146 Genova, Italy

Received May 30, 1989/Accepted in revised form October 3, 1989

Abstract. Ionic and gating currents from voltage-gated sodium channels were recorded in mouse neuroblastoma cells using the path-clamp technique. Displacement currents were measured from whole-cell recordings. The gating charge displaced during step depolarizations increased with the applied membrane potential and reached saturating levels above 20 mV. Prolonged large depolarizations produced partial immobilization of the gating charge, and only about one third of the displaced charge was quickly reversed upon return to negative holding potentials. The activation and inactivation properties of macroscopic sodium currents were characterized by voltage-clamp analysis of large outside-out patches and the single-channel conductance was estimated from non-stationary noise analysis. The general properties of the sodium channels in mouse neuroblastoma cells are very similar to those previously reported for various preparations of invertebrate and vertebrate nerve cells.

Key words: Sodium channel – Gating currents – Mammalian cells – Patch clamp

Introduction

Sodium channels are among of the most important structures of excitable cells in higher animals. Their presence allows the development of electrically stimulated action potentials, provided the cell membrane is polarized at rest by some parallel ion permeation mechanism. The opening of the sodium channels is modulated by the membrane potential because it involves conformational changes of the channel proteins which are accompanied by charge movements in the direction perpendicular to the membrane. These charge translocations are directly observable as tiny asymmetric displacement currents, called gating currents, mostly preceding the opening of the channels after a depolarizing step of membrane potential.

Sodium gating currents were first observed in squid giant axons (Armstrong and Bezanilla 1974; Keynes and Rojas 1974) and later also in other nerve preparations, such as the node of Ranvier of the frog (Nonner et al. 1975; Neumcke et al. 1976; Dubois and Schneider 1982), the giant axons of Myxicola (Bullock and Shauf 1978) and crayfish (Starkus et al. 1981), and *Aplysia* neurons (Adams and Gage 1979). Also a small fraction of the asymmetric displacement currents in skeletal muscle fibers is attributed to sodium gating currents (Almers 1978). No such measurement has been so far reported for mammalian neurons or for cultured cells studied with the patch recording technique.

We have recorded ionic and gating currents in mouse neuroblastoma cells, a preparation which shows a high density of sodium channels. We have found that measurements of current fluctuations and gating currents can be easily performed on cultured cells using the patch-clamp technique (Hamill et al. 1981). The properties of sodium channels of mammalian neurons appear to be in all respects similar to those of other preparations.

Methods

Cell preparation

The experiments were performed on the Neuroblastoma cell line NE41A3 from the mouse. The cells were plated on untreated plastic Petri dishes, and could be used within 24 to 48 h after preparation. The solution used in the cell bath was (in millimolar): NaCl 160, $CaCl_2$ 2, $MgCl_2$ 1, HEPES-NaOH (*N*-2-Hydroxyethylpiperazine) 10. The pipette solution, dialyzing the intracellular compartment was: CsF 110, NaCl 10, EGTA 11 (Ethylenglycol-*bis*-β-amino-ethylether), HEPES-NaOH 10. In both solutions the pH was adjusted to 7.4. All measurements were performed at room temperature (24 to 25 °C).

Offprint requests to: O. Moran

Voltage clamp experiments

Recordings from whole-cells and from membrane patches in the outside-out configuration were obtained according to the methods described by Hamill et al. (1981) using a standard patch-clamp amplifier (EPC-7, List Medical Electronics, Darmstadt, FRG). Patch recordings were used to characterize sodium ion currents. Gating currents were recorded from whole-cells using borosilicate glass pipettes with resistances in the range 1 to 2 Mohm. For the latter measurements the cells were gently detached from the Petri-dish before being approached with the recording pipette and only those cells which showed maximal peak inward currents larger than 3 nA were selected. After checking for the existence of this condition, the sodium currents were blocked by addition of 2.2 μM-TTX (Tetrodotoxin, Sigma, St. Louis). Raising the TTX concentration to 5 μM made no difference to the results. In all experiments potassium currents were absent because of the intracellular substitution of K^+ with Cs^+. Calcium currents were also insignificant, as demonstrated by the absence of any appreciable effect of 2.5 mM cadmium or 5 mM cobalt ions, known to be very potent blockers of calcium channels (Brown et al. 1981; Carbone and Lux 1984). In all cases most of the linear component of the membrane current in response to a voltage-step stimulation was compensated analogically. The full correction of the capacitive and leak responses was made digitally off-line depending on the exact protocol used for the various measurements (ionic currents and gating currents, current fluctuations), described below. The holding potential was maintained at -90 mV.

Data acquisition and analysis

The stimulation and data acquisition were controlled by a minicomputer (PDP-11/23, Indec, Sunnyvale, Ca) programmed in Brown-BASIC. Before digital acquisition the output of the patch-clamp amplifier was filtered by a low-pass 4-pole Bessel filter (Ithaco, 4302) set at a cut-off frequency of 10 kHz. The membrane current was sampled every 10 μs.

Standard pulse protocols were used to study the macroscopic properties of the sodium current, $I(t)$. A series of voltage pulses to various depolarizing levels between -60 and 80 mV yielded the voltage dependence of activation and that of activation and inactivation kinetics. Double-pulse stimulations comprising a fixed test pulse preceded by a conditioning prepulse to various voltage levels allowed us to characterize the voltage dependence of the steady-state sodium inactivation. All stimulations for $I(t)$ measurements were followed by a similar pulse protocol in which the pulse amplitudes were reduced to 1/4 and the holding potential was brought to -120 (P/4 procedure, see Armstrong and Bezanilla 1974). The P/4 responses were used to subtract the linear membrane response from the total measured current.

The stimulation protocol for gating current measurements consisted of several groups of 8 repetitions of step depolarizations from a conditioning 5 ms prepulse to -100 mV to various test potentials. Each repetition was followed by a P/4 protocol with a holding potential of -120 to -160 mV.

Non-stationary noise measurements were obtained from the analysis of ensemble averages over a large number of responses to identical test pulses (Sigworth 1977). The ensemble of records collected in any experiment consisted of alternating groups of 20 responses to test stimulations and 5 responses to control pulses. Test records were obtained by pulsing to potentials between 0 mV from the holding potential of -90 mV. Control stimuli consisted of hyperpolarizing pulses of 20 mV amplitude and identical temporal pattern. Individual pulses were applied consecutively every 1.5 s, and the alternating sequences were automatically chain-repeated until the series was interrupted by hand. Differences between two successive test records were used for the analysis of the fluctuations (Conti et al. 1980). Difference records were squared and averaged to yield an estimate of twice the variance of $I(t)$. The average of the responses to each test pulse was appropriately corrected for the linear component derived from the average response to the control pulses to yield an estimate of the mean $I(t)$. Variance vs. mean plots yielded estimates of the current flowing through a single open channel at the test voltage and of the number of sodium channels active under the recording pipette during the measurement.

Results

Sodium currents

Figure 1 A shows a series of sodium current responses, $I(t)$, evoked by step depolarizations to membrane potentials, V_m, in the range -80 to 50 mV in an excised membrane patch of a neuroblastoma cell in the outside-out configuration (Hamill et al. 1981). Each trace is the average of 4 original records and is corrected for linear leakage and capacitive transients using the P/4 procedure as described in Methods. The membrane patch, obtained using a pipette with a series resistance $R_s = 1.2$ M ohm, presumably had an area larger than 10 μm^2 and contained several hundreds of sodium channels which accounts for the large size of the recorded currents. Such large patches allow an accurate characterization of macroscopic sodium currents with no significant contamination of the recordings due to R_s. Series resistance artifacts can be as serious a problem in whole-cell recordings from large cells as in the squid axon preparation where they were first described (Hodgkin et al. 1952). In the case of the records of Fig. 1 the lack of R_s compensation may have caused variations in the voltage actually applied across the membrane patch of at most 0.5 mV.

Figure 1 B shows a plot of the peak current, I_p, as a function of the applied voltage. I_p was estimated from least-squares fits of experimental records in a short interval around the peak with a third order polynomial. The reversal potential, E_r, i.e. the applied voltage for which I_p changes sign, is estimated in this patch to be about 54 mV,

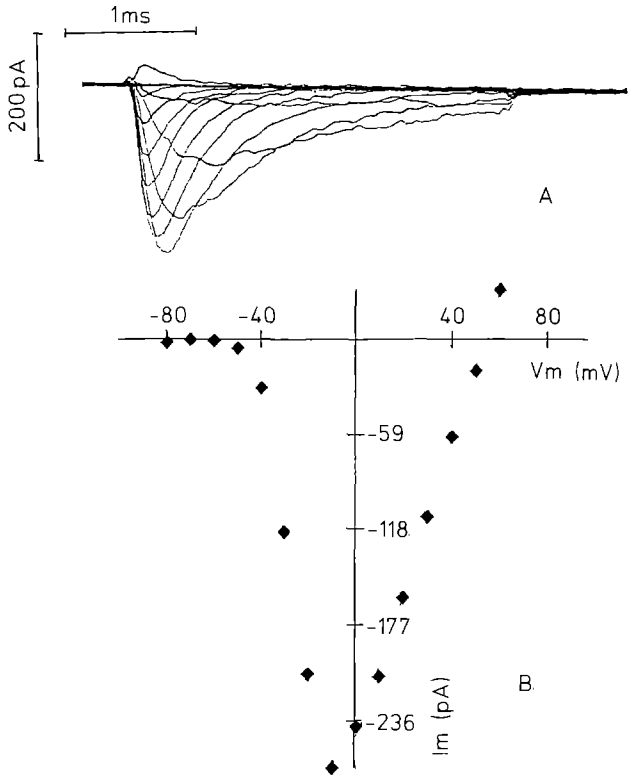

Fig. 1. **A** Sodium currents from an outside-out patch of a mouse neuroblastoma cell. The holding potential was −90 mV, and the test pulses were from −80 to 60 mV. Each trace is an average of 4 records. **B** Peak current, I_p vs. voltage relationship. I_p is maximal (260 pA) around −8 mV and the reversal potential is about 54 mV. Temperature 24 °C. Experiment 1NE14

Table 1. Activation fit parameters. V_m^o is the half activation potential, z_m is the apparent valence of a single activation process, V_h^o is the half inactivation potential, a_h is the inactivation voltage dependence and I_{min} is the peak current

File	V_m^o [mV]	z_m	V_h^o [mV]	a_h [mV]	I_{min} [pA]
1NE06	−37.4	1.54	−71.7	11.1	−264
1NE07	−35.6	2.03	−77.5	11.0	−159
1NE14	−37.1	1.58	−71.0	11.4	−260
1NE15	−37.3	1.71	−77.6	11.0	−157
mean:	−36.9	1.72	−74.5	11.1	−264
s.d.:	0.8	0.22	3.6	0.2	52.0

very close to the Nernst equilibrium potential for sodium ions ($[Na^+]_o = 170$ mM, $[Na^+]_i = 20$ mM).

A more detailed analysis of the voltage-clamp responses was made according to the Hodgkin-Huxley (HH) equations (Hodgkin and Huxley 1952) with the addition of an empirical delay, δt, in the onset of the classical $m^3 h$ kinetics (Keynes and Rojas 1976). The fitting of each current trace proceeded as follows. The late phase of $I(t)$ was least-squares fitted with a function, $I_i(t)$, consisting of a single exponential decay to a stationary level that was significant only for responses to moderate depolarizations (−60 to −40 mV in Fig. 1 A). The time constant of $I_i(t)$, τ_h, characterizes the kinetics of the inactivation of the sodium currents. The voltage dependence of τ_h for a typical measurement in our cell preparation is shown in Fig. 2 A (triangles). The activation time constant, τ_m was obtained from the least-squares fit of the rising phase of $I(t)/I_i(t)$ to the function:

$$I(t)/I_i(t) = (1 - \exp(-(t-\delta t)/\tau_m))^3$$

With the holding potential of −90 mV used in most of our measurements the fit values of δt typically ranged between zero and 40 μs, and decreased with voltage for $V_m > -10$ mV. τ_m data for the same patch that yielded the τ_h data of Fig. 2 A are shown in the same figure as diamonds.

Assuming that both activation and inactivation occur with the same delay, $I_i(\delta t)$ was taken as the asymptotic current level, I', that would be approached at long times if the inactivation process were absent. Assuming a linear voltage dependence of the current flowing through an open sodium channel, the asymptotic conductance, $G' = I'/(V - E_r)$, is proportional to the asymptotic open channel probability, m_∞^3. G' data for the same patch of Fig. 2 A are shown in Fig. 2 B. The smooth line through the experimental points is the least-squares fit of the data assuming a voltage-dependence of m_∞ of the type:

$$m_\infty(V) = 1/\left(1 + \exp\left(\frac{z_m e_0 (V - V_m^0)}{k T}\right)\right) \quad (1)$$

where e_0 is the electron charge (-1.6×10^{-19} Coulomb), k is Boltzmann's constant and T is the absolute temperature. The fit parameters used in Fig. 2 B are typical for our mammalian cells (see also Table 1). The half activation voltage, V_m^0 was −37 mV; the apparent valence of a single activation process (m-gate), z_m, was 1.6.

The voltage dependence of the steady-state sodium inactivation parameter, h_∞, is shown in Fig. 2 C. h_∞ data were obtained from the measurement of the peak currents in response to test pulses to −10 mV, following conditioning prepulses of 60 ms duration to various voltages, V_p. The smooth line through the data is the least-squares fit assuming a voltage dependence of h_∞ of the type:

$$h_\infty(V_p) = 1/\left(1 + \exp\left(\frac{V_p - V_h^0}{a_h}\right)\right) \quad (2)$$

For the data of Fig. 2 C the fit value of the half-inactivation potential, V_h^0, was −71 mV, and the steepness of the voltage dependence was characterized by $a_h = 11$ mV. Estimates of V_h^0 and a_h from other experiments are given in Table 1.

Estimate of the single-channel conductance

In order to characterize the properties of the single-channel events responsible for the above described macroscopic currents, we measured the variance of the current fluctuations in three excised patches. This allowed us to obtain estimates of both the number, N, of activable sodium channels present in the patch and of the current, i, flowing through a single open channel at a given mem-

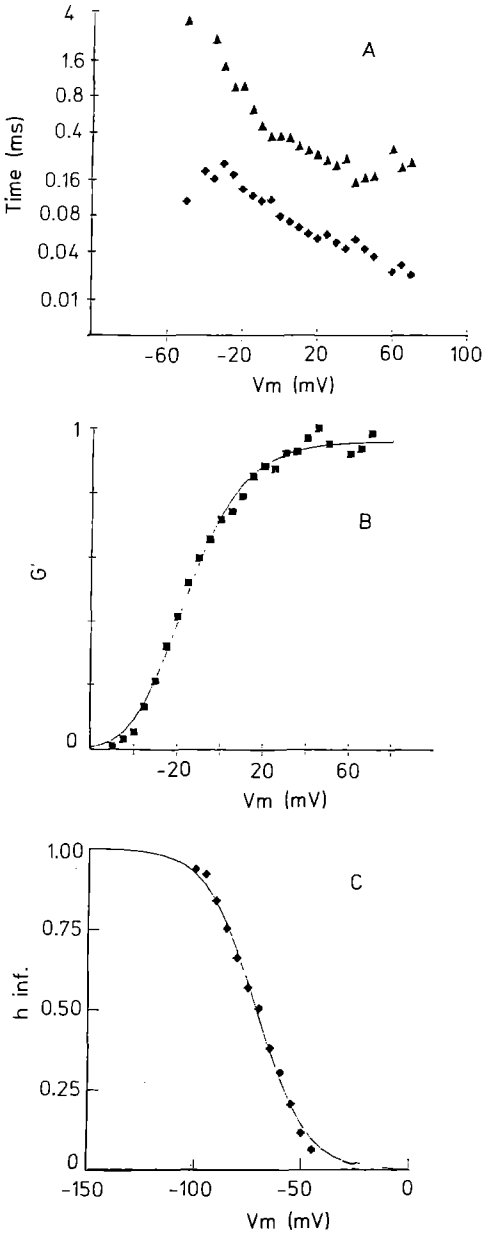

Fig. 2 A–C. Hodgkin-Huxley analysis of the sodium currents in an outside-out patch of mouse neuroblastoma cell. **A** Voltage dependence of the activation and inactivation time constants, τ_m and τ_h. **B** Voltage dependence of the apparent asymptotic sodium conductance, G', estimated as described in the text. The continuous line shows the least-squares fit of the data to the expression $G_0 m_\infty^3$, with m_∞ given by (1) and $G_0 = 13.7$ nS, $V_m = -37$ mV, $z_m = 1.6$. **C** Voltage dependence of the inactivation parameter, h_∞, was measured as described in the text. The continuous line shows the least-squares fit of the data according to (2) with $V_h = -71$ mV and $a_h = 11$ mV. Temperature 24 °C. Experiment 1NE14

brane potential, according to the equation (Sigworth 1977):

$$\sigma^2(t) = \sigma_b^2 + i\, I(t)\left(1 - \frac{I(t)}{N\, i}\right) \qquad (3)$$

where $\sigma^2(t)$ is the variance, $I(t)$ is the mean of the sodium currents produced by repeated identical voltage-step stimulations and σ_b^2 is the background noise variance.

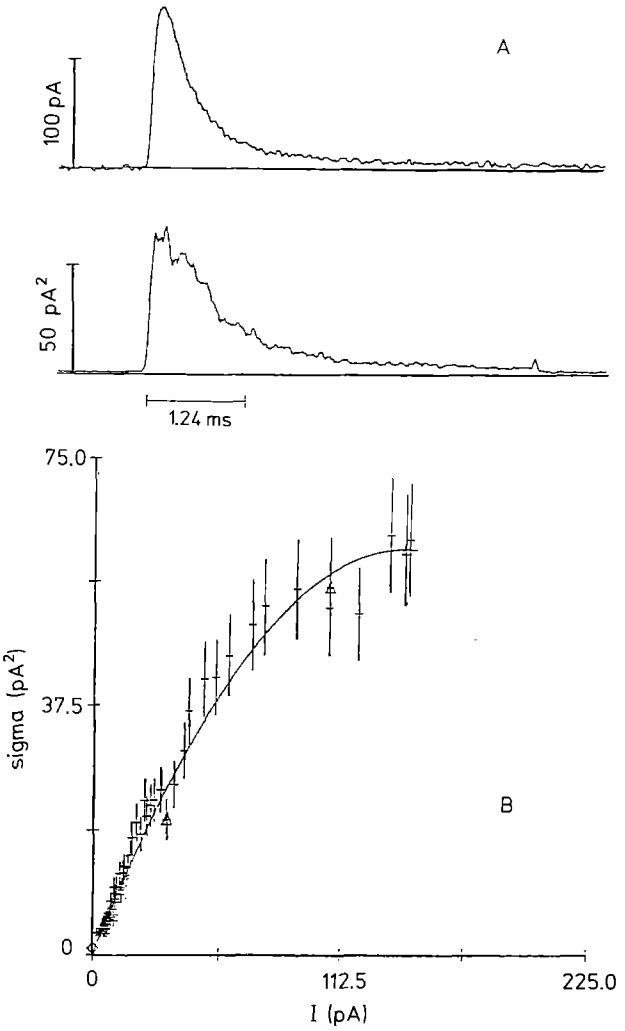

Fig. 3 A, B. Fluctuation analysis of the sodium current in an outside-out membrane patch of a mouse neuroblastoma cell. **A** Comparison between the average current, $I(t)$, and the average squared-fluctuation, σ_I^2, of the sodium currents elicited by 124 successive test depolarizations at 0 mV from the holding potential of −90 mV. **B** Plot of the variance vs. mean data shown in **A** during the pulse interval. For convenience of display the data are shown condensed in bins obtained by dividing the $I(t)$ values into 75 equal intervals. The error bars represent ± standard errors, estimated according to the measured variance and taking into account both the number of trials used for estimating the mean and the variance and the number of data points in each bin. The continuous line is the weighted least-squares fit of the plot according to (3), yielding $i = 0.85$ pA, $N = 334$, and $\sigma_b^2 = 1.1$ pA^2. Recording bandwidth 10 kHz. Temperature 24 °C. Experiment N1NE15

Figure 3 shows the results of this type of analysis for one experiment in which an excised patch was exposed to 124 identical test voltage pulses to 0 mV from a holding potential of −90 mV. Figure 3 A (upper panel) shows the mean current response corrected for leakage and capacitive transients as described in Methods. The averages obtained from the first 20 and from the last 20 trials of the series were not appreciably different from the overall mean, showing that the response was stable during the 5 min period of the whole measurement. In all fluctuation measurements reported here the decay of the mean cur-

Table 2. Estimates of single-channel currents obtained by fluctuation analysis at a test potential pulse of 0 mV. V_r is the reversal potential, i is the single channel current, γ is the single channel conductance, N is the number of sodium channels under the patch pipette and N_T is the number of trials in each experiment

File	V_r [mV]	i [pA]	γ [pS]	N	N_T
N1NE06	53	0.86	16.2	422	144
N1NE15	53	0.85	16.1	334	124
N2NE05	55	0.94	17.2	380	98
		mean:	16.5 (±0.6)		

rent at the end of a run was less than 2%. The difference method guarantees that a run-down of this extent does not interfere significantly with the variance estimates (Conti et al. 1980). Figure 3B (lower panel) shows the time course of the variance of the recorded currents without any correction for σ_b^2. It is seen that σ_b^2, as measured before the onset of the voltage pulse stimulation, is trivially small in comparison to the variance of the current fluctuations during the pulse. The least-squares fit of the plot of the variance versus the mean of the sodium current is shown in Fig. 3B. For convenience in the illustration, the data in Fig. 3B are presented lumped into 75 bins of mean current values. The bars give ± standard errors, estimated from the actual variance data and taking into account the number of samples used. The smooth line is the weighted least-squares fit of the data according to (3).

Since E_r was 53 mV in this patch, the i estimate implies a single-channel chord-conductance, $\gamma \approx 16$ pS, close to the values obtained from single-channel recordings in several other preparations (Sigworth and Neher 1980; Fendwick et al. 1982; Stühmer et al. 1987).

In the experiment of Fig. 3, the area of the patch was estimated to be about 15 μm² (from the measured capacity of the patch and assuming a membrane specific capacity of 1 μF/cm²). This yields an estimate of about 25 channels per μm². Considering that the single channel current at the voltage at which the maximum I_p values are obtained ($V_m \approx -10$ mV) is ≈1 pA, and assuming an open channel probability of 0.5 at $V_m = -10$ mV, such channel density predicts a maximal value for I_p of:

$$I_p^{\max} = N\, p\, i\, s$$

where s is the cell membrane surface. For a cell of 10 μm diameter we expect $I_p^{\max} = 4$ nA, which compares well with the value measured in the whole configuration before excising the patch.

The results of noise measurements performed on 3 different patches are summarized in Table 2. The γ estimates have a mean value of 16.5 pS and lie in the narrow range of 16 to 18 pS, while I_p in whole-cell current records varies by more than a factor of 5 due to variations in cell diameter and channel density. N estimates vary in a wider range, presumably because of intrinsic variability of this quantity, which depends on the patch area, but also perhaps because of the much lower accuracy of N estimates with this method. On the other hand, the small scatter of γ estimates rules out possible artifacts which should produce variances increasing with the square of the signal rather than roughly linearly with I_p as found in agreement with (3).

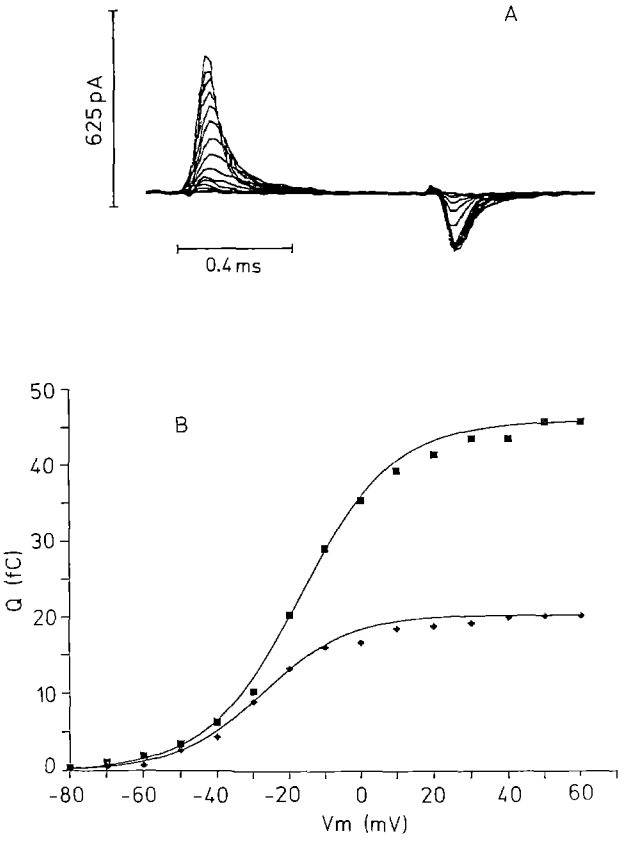

Fig. 4. **A** Sodium gating currents, I_g, recorded from a whole neuroblastoma cell after blocking the ionic currents with 2.2 μM TTX. The I_g's were elicited by 1 ms depolarizing test pulses to membrane potentials in the range −80 to 60 mV, increasing in steps of 20 mV, following a 5 ms prepulse to −100 mV. The cell area was about 500 μm², so that we expect from our estimates of channel density to have about 12,500 channels. **B** Voltage dependence of the gating charges, Q_{on} (squares) and Q_{off} (diamonds), displaced respectively during the onset and during the early phase of the offset of the test pulse. The continuous line shows the least-squares fit of the Q_{on} data according to (4), with $Q_o = 45.7$ fC, $V_g = -16.6$ mV and $z_g = 1.97$. Recording bandwidth 10 kHz. Temperature 24 °C. Experiment 1Ne11

Gating currents

When the sodium currents were blocked with TTX, the linear transient subtraction according to the procedure described in Methods left an uncompensated component of the current responses to depolarizing pulses which carried a saturable charge displacement with all the standard features of sodium gating currents (reviewed by Almers 1978). Figure 4A shows a family of average asymmetric displacement currents, $I_g(t)$, recorded from a cell that produced a maximum ionic current of 11 nA at −10 mV before TTX treatment. The applied test pulses brought the membrane potential from the prepulse level of −100 mV to various levels, V, between −80 mV and 60 mV in steps of 10 mV. The responses were recorded

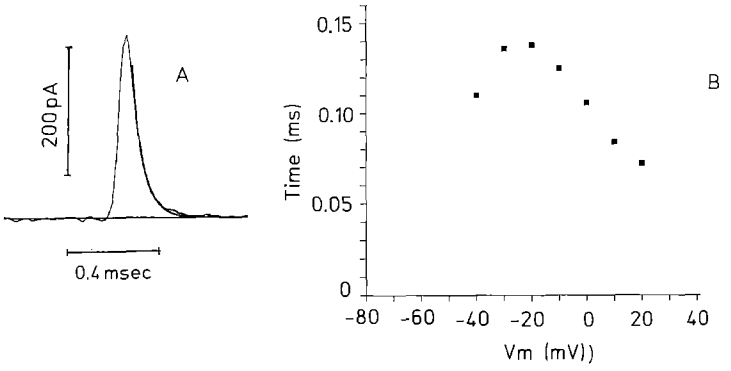

Fig. 5 A, B. Voltage dependence of gating current kinetics. **A** Fit of the decay of gating current recorded at 40 mV with a single exponential. The time constant, τ_{on}, is plotted in **B** as a function of the membrane potential applied during the test pulse. Temperature 24 °C. Experiment 1NE11

Table 3. Total charge, Q_o, V_g and single-gate charge, z_g

File	Q_o [fC]	V_g [mV]	z_g
1NE07	27.6	−23.8	2.39
1NE11	45.7	−16.6	1.97
1NE11A	42.5	−31.0	2.19
1NE12	39.8	−20.3	1.88
2NE05	26.7	−18.4	1.98
2NE06	51.3	−21.4	1.83
2NE05A	32.8	−17.5	2.03
	mean:	−21.3 (±5.0)	2.04 (±0.19)

with a bandwidth of 10 kHz. The membrane capacity of this cell was about 8 pF and the pipette resistance 1.2 M ohm, and no R_s compensation was used, so that the voltage-clamp had an effective time constant of about 10 μs.

For each average record the total gating charge displaced after the onset of the test pulse, Q_{on}, and that recovered during the early phase of the repolarization, Q_{off}, were measured by integrating $I_g(t)$ over the appropriate time intervals. Plots of Q_{on} (squares) and Q_{off} (diamonds) vs. V are shown in Fig. 4B. The gating current data of Fig. 4 are very similar to those obtained from squid axons (Armstrong and Bezanilla 1974; Keynes and Rojas 1976) and frog nodes of Ranvier (Neumcke et al. 1976).

The Q_{on} values of Fig. 4B reach a saturating level of about 46 fC at potentials higher than 20 mV. The continuous line in Fig. 4B is a least-squares fit of the Q_{on} data according to the following Eq.:

$$Q_{on} = Q_o / \left(1 + \exp\left(-z_g e_0 \frac{(V - V_g)}{k T}\right)\right) \quad (4)$$

with: $Q_o = 45.7$ fC, $V_g = -16.6$ mV, and $z_g = 1.97$. Equation (4) gives the theoretical voltage dependence of the gating charge for a system of independent two-state gates in which two conformations of a single gate have an effective transmembrane charge distribution difference $z_g e_0$ (Keynes and Rojas 1976; Schwarz 1978; Conti 1986). Values of Q_o, V_g, and z_g from 7 different experiments are given in Table 3.

It is clear from Fig. 4B that Q_{on} is always higher than Q_{off}. The ratio Q_{on}/Q_{off} increases with increasing test pulse depolarizations. It was also observed (not shown) that the above ratio increased with the duration of the test pulse. This is a well characterized standard feature of the sodium gating currents which is due to the partial immobilization of the gating transitions caused by the process of inactivation of the sodium channel (Armstrong and Bezanilla 1977; Neumcke et al. 1976). In agreement with squid axon and frog node data we find that inactivation immobilizes up to 2/3 of the gating charge, as shown by the comparison of the saturating levels of Q_{on} and Q_{off} in Fig. 4B.

The decay of $I_g(t)$ was well fitted by a single exponential for voltages in the range −40 to 20 mV, which produced large enough currents with time constants, τ_{on}, readily measurable with our recording bandwidth. Figure 5 shows examples of the fit and a plot of τ_{on} as a function of membrane potential in a particular experiment on a single cell. τ_{on} reached a maximum value of about 140 μs around −25 mV. Both these values are in fair agreement with previous measurements in the squid axon (Keynes and Rojas 1974), in the frog node (Nonner et al. 1975; Dubois and Schneider 1982), and in *Myxicola* neurons (Bullock and Shauff 1978). In these preparations the reported values of the maximal τ_{on} range from 230 μs to 500 μs, at temperatures 12 to 20 °C lower than ours.

Discussion

The direct characterization of sodium channels from single-channel current recordings (Sigworth and Neher 1980; Aldrich et al. 1983; Horn and Vandenberg 1984) requires the collection and analysis of large amounts of single-channel data from selected membrane patches containing only few active channels, ideally a single one. Such experimental conditions are particularly difficult to achieve in neurons which have a high density of sodium channels as in the case of our neuroblastoma cells. On the other hand, the presence of a large number of channels in the membrane sets ideal conditions for accurate measurements of macroscopic currents which can be rich in information. These measurements include fluctuation analysis, yielding information about single-channel currents, and gating currents, which are impossible to detect at the single-channel level.

Although less directly translatable into molecular mechanisms, the macroscopic analysis provides enough

experimental data to fit any reasonable model of channel gating containing a limited number of parameters. The main purpose of the present work was to show that a full characterization of macroscopic sodium currents can be obtained in cultured neurons using the patch-clamp recording technique. In general our results confirm the notion that neuroblastoma sodium channels behave in a manner typical of other preparations (Moolenar and Spector 1977; Huang et al. 1982), with the additional support derived from our novel gating current data.

By fitting the kinetic and steady-state properties of the macroscopic sodium currents recorded from excised patches according to the HH equations (Hodgkin and Huxley 1952), we have obtained a phenomenological description of the sodium permeability in our cultured mammalian cells which allows a quantitative comparison with other preparations. In particular, our results are in good agreement with those reported for the rat node (Neumcke and Stämpfli 1982), which is the native preparation closest to ours, and for the sodium currents expressed by frog oocytes after injection of the mRNA coding for rat brain sodium channels (Stühmer et al. 1987). We find that the voltage-dependencies of the HH parameters m_∞ and τ_m are slightly different from those of the analogous gating current parameters Q_{on} and τ_{on}. While differences between z_m and z_g lie within experimental errors, the $m_\infty - V$ and $\tau_m - V$ curves seems to be more systematically shifted (≈ 15 mV toward more negative potentials) with respect to $Q_{on} - V$ and $\tau_{on} - V$ curves. It is possible that such a shift is due to the difference in recording conditions (outside-out patches for ionic currents as opposed to whole-cell for gating currents) as suggested by the finding that excision of membrane patches shifts the inactivation of sodium channels in the patches (Nilius 1988). However, we could not directly confirm this interpretation because the large ionic current densities in our preparation prevent reliable space- and voltage-clamp conditions in the whole-cell configuration.

The single-channel conductance estimates from our noise measurements are about twice as large as those obtained in squid giant axons and frog nodes (reviewed by Conti 1984), but in good agreement with estimates from mammalian nodes (Neumcke and Stämpfli 1982). As discussed in detail by the latter authors most of the differences in γ estimates are accountable for by the higher temperature and extracellular sodium concentration that they and we used in our experiments. Our data agree quantitatively also with single-channel recordings in cultured rat muscle cells (Sigworth and Neher 1980), in the rat pituitary cell line GH_3 (Horn and Vandenberg 1984), in the rat neuroblastoma cell line N1E115 (Aldrich et al. 1983), and in frog oocytes injected with rat brain sodium-channel-mRNA (Stühmer et al. 1987).

According to the currently accepted notion, the classical HH-scheme is not a faithful picture of the molecular events underlying the gating of sodium channels. In particular the description of inactivation as an independent process is unrealistic. Indeed, both gating-current and single-channel measurements show that the inactivating transition depends on the state of activation (Armstrong and Bezanilla 1977; Aldrich et al. 1983). The strongest evidence of activation-inactivation coupling is the immobilization of two thirds of the gating charge when the sodium channels are fully inactivated (Armstrong and Bezanilla 1977). We have confirmed the latter result in our gating current measurements on mammalian cells. Indeed, all the features of the gating currents that we have recorded from our preparation closely resemble those previously described in other preparations.

Acknowledgements. O. M. was recipient of a fellowship from the International Center of Theoretical Physics, Trieste, Italy within the Programme for Research in Italian Laboratories.

References

Adams DJ, Gage PW (1979) Sodium and calcium gating currents in an *Aplysia* neuron. J Physiol 291:467–481

Aldrich RW, Corey DP, Stevens CF (1983) A reinterpretation of mammalian sodium channel gating based on single channel recording. Nature 306:436–441

Almers W (1978) Gating and charge movements in excitable membranes. Rev Physiol Biochem Pharmacol 82:96–190

Armstrong CM, Bezanilla F (1974) Charge movement associated with the opening and closing of the activation gates of the Na channels. J Gen Physiol 63:533–552

Armstrong CM, Bezanilla F (1977) Inactivation of the sodium channel. II. Gating current experiments. J Gen Physiol 70:567–590

Brown AM, Murimoto K, Tsuà Y, Wilson DL (1981) Calcium current-dependent and voltage-dependent inactivation of calcium channels in *Helix aspersa*. J Physiol 320:193–218

Bullock JO, Schauf CL (1978) Combined voltage-clamp and dialysis of *Myxicola* axons: behaviour of membrane asymmetry currents. J Physiol 278:309–324

Carbone E, Lux HD (1984) A low voltage activated, fully inactivated Ca channels in sensory neurons. Nature 310:501–502

Conti F (1984) Noise analysis and single-channel recordings. Curr Top Membr Transp 22:371–405

Conti F (1986) The relationship between electrophysiological data and thermodynamics of ion channel conformations. Neurol Neurobiol 20:25–41

Conti F, Neumcke B, Nonner W, Stämpfli R (1980) Conductance fluctuations from the inactivation process of sodium channels in myelinated nerve fibers. J Physiol 308:217–239

Dubois JM, Schneider MF (1982) Kinetics of intramembrane charge movement and sodium current in frog node of Ranvier. J Gen Physiol 79:571–602

Fenwick EM, Marty A, Neher E (1982) Sodium and calcium channels in bovine chromaffin cells. J Physiol 331:599–635

Hamill OP, Marty A, Neher E, Sakmann B, Sigworth FJ (1981) Improved patch-clamp techniques for high resolution current recording from cells and cell-free membrane patches. Pflügers Arch 391:85–100

Hodgkin AL, Huxley AF (1952) A quantitative description of membrane current and its application to conduction and excitation in nerve. J Physiol 117:500–544

Hodgkin AL, Huxley AF, Katz B (1952) Measurement of current-voltage relations in the membrane of the giant axon of *Loligo*. J Physiol 116:424–448

Horn R, Vandenberg CA (1984) Statistical properties of single sodium channels. J Gen Physiol 84:505–534

Huang LM, Moran N, Ehrenstein G (1982) Batrachotoxin modifies the gating kinetics of sodium channels in internally perfused neuroblastoma cells. Proc Natl Acad Sci USA 79: 1082–2085

Keynes RD, Rojas E (1974) Kinetics and steady-state properties of the charged system controlling sodium conductance in the squid giant axon. J Physiol 239:393–434

Keynes RD, Rojas E (1976) The temporal and steady-state relationships between activation of the sodium conductance and movement of the gating particles in the squid giant axon. J Physiol 255:157–189

Moolenaar WH, Spector I (1977) Membrane currents examined under voltage-clamp in cultured neuroblastoma cells. Science 196:331–333

Neumcke B, Stämpfli R (1982) Sodium currents and sodium-current fluctuations in rat myelinated nerve fibers. J Physiol 329: 163–384

Neumcke B, Nonner W, Stämpfli R (1976) Asymmetrical displacement current and its relation to the activation of sodium current in the membrane of frog myelinated nerve. Pflügers Arch 363:193–203

Nilius B (1988) Modal gating behavior of cardiac sodium channels in cell-free membrane patches. Biophys J 53:857–862

Nonner W, Rojas E, Stämpfli R (1975) Displacement currents in the node of Ranvier. Voltage and time dependence. Pflügers Arch 354:1–18

Schwarz G (1978) On the physico-chemical basis of voltage-dependent molecular gating mechanisms in biological membranes. J Membr Biol 43:127–148

Sigworth FJ (1977) Sodium channels in nerve apparently have two conductance states. Nature 270:265–267

Sigworth FJ, Neher E (1980) Single Na^+ channel current observed in cultured rat muscle cells. Nature 287:447–449

Starkus JG, Fellmeth BD, Rayner MD (1981) Gating currents in the intact crayfish giant axon. Biophys J 35:521–533

Stühmer W, Methfessel C, Sakmann B, Noda M, Numa S (1987) Patch clamp characterization of sodium channels expressed from rat brain cDNA. Eur Biophys J 14:131–138